

# Cotunneling current through quantum dots with phonon-assisted spin-flip processes

Jörg Lehmann\* and Daniel Loss

*Department of Physics and Astronomy, University of Basel,  
Klingelbergstrasse 82, CH-4056 Basel, Switzerland*

(Dated: November 7, 2018)

We consider cotunneling through a quantum dot in the presence of spin-flip processes induced by the coupling to acoustic phonons of the surrounding. An expression for the phonon-assisted cotunneling current is derived by means of a generalized Schrieffer-Wolff transformation. The influence of the spin-phonon coupling on the heating of the dot is considered. The result is evaluated for the case of a parabolic semiconductor quantum dot with Rashba and Dresselhaus spin-orbit coupling and a method for the determination of the spin-phonon relaxation rate is proposed.

PACS numbers: 73.21.La, 05.60.Gg, 72.25.Rb, 03.65.Yz

## I. INTRODUCTION

In the past years, prospective applications in spintronics and quantum computation<sup>1,2,3,4</sup> have lead to a growing interest in the magnetic properties of nanoscale systems. A variety of systems ranging from semiconductor quantum dots over molecular magnets<sup>5,6,7,8,9</sup> down to single atoms on surfaces have been studied in detail.<sup>10,11</sup> For the investigation of such systems, transport measurements provide an excellent tool. Recently, the Zeeman splitting of two spin-levels has been measured via inelastic tunneling spectroscopy, both in GaAs quantum dots<sup>12</sup> and in single Mn atoms on a surface which have been addressed by an STM tip.<sup>10</sup> Using the same technique, the singlet-triplet splitting in few-electron quantum dots has been determined.<sup>13</sup>

For the applications mentioned at the beginning it is crucial that effects like relaxation and the loss of quantum coherence resulting from the coupling of the nanosystem to its surrounding environment are sufficiently weak. In particular, a detailed knowledge about these effects is a prerequisite for the assessment of the suitability of a specific system for application purposes. In the case of the electron spin in semiconductor quantum dots, relaxation at low magnetic fields is dominated by the hyperfine coupling to the nuclei,<sup>14,15,16</sup> while at higher fields the spin-orbit interaction induced coupling to acoustical phonons is most relevant.<sup>17,18</sup> It turns out that both effects are sufficiently weak, and correspondingly long spin-relaxation times have been reported.<sup>19,20,21</sup> For the single-atom experiments reported in Ref. 10, the strength of different coupling mechanisms is not yet clear, however, and the measurement schemes which were used in the semiconductor case are not directly applicable.

In the present work, we study to what extent inelastic cotunneling spectroscopy can yield information about intrinsic spin-flip processes due to a coupling to bosonic degrees of the freedom in the surrounding. We put forward a general approach for the calculation of the cotunneling current<sup>22,23</sup> in the presence of such spin-flip processes. Subsequently, we apply the general formalism to the case of cotunneling across GaAs/AlGaAs semiconductor quantum dots and propose a method for the

determination of the spin-relaxation rate.

The outline of the present work is as follows. In Sec. II, we start by introducing the model for the quantum dot coupled via a tunneling Hamiltonian to two fermionic leads and via a spin-phonon coupling to a bosonic environment. In the next section, we put forward a generalized Schrieffer-Wolff transformation, which, in the limit of a weak spin-phonon coupling, allows one to eliminate to lowest order the dot-lead coupling. We then derive, in Sec. IV, expressions for the elastic and inelastic cotunneling current in the presence of the spin-phonon coupling. For the evaluation of the current, the knowledge of the occupation probabilities of the spin-states on the dot is required. Their dynamics is governed by a master equation, which is discussed in Sec. V. The experimentally most relevant quantity, the differential conductance as a function of the bias voltage, is evaluated in Sec. VI. In Sec. VII, we apply the general result to a realistic model describing a recent experiment by Kogan et al. (Ref. 12). Sec. VIII briefly discusses the low-temperature behavior. The final conclusions are presented in Sec. IX.

## II. MODEL

We consider transport across a quantum dot in a spin-1/2 ground-state contacted to two leads in the presence of an intrinsic spin-flip mechanism due to the coupling of the dot to a phonon bath (see Fig. 1). The total system consisting of dot, leads and phonons is described by the Hamiltonian

$$H = H_0 + H_T + H_S. \quad (1)$$

Here,  $H_0$  is the Hamiltonian of the isolated dot, the ideal leads  $\ell = L, R$  and the phonons, i.e.,

$$H_0 = \sum_{\sigma=\uparrow,\downarrow} E_\sigma n_\sigma + U n_\uparrow n_\downarrow + \sum_{\ell\mathbf{k}\sigma} \epsilon_{\ell\mathbf{k}} n_{\ell\mathbf{k}\sigma} + \sum_{\mathbf{q}} \hbar\omega_{\mathbf{q}} n_{\mathbf{q}}. \quad (2)$$

The number operator of the dot spin is given by  $n_\sigma = d_\sigma^\dagger d_\sigma$ , where  $d_\sigma$  ( $d_\sigma^\dagger$ ) destroys (creates) an electron with spin  $\sigma = \uparrow, \downarrow$  on the dot. An externally applied magnetic field  $B_z$  in z-direction leads to a Zeeman splitting

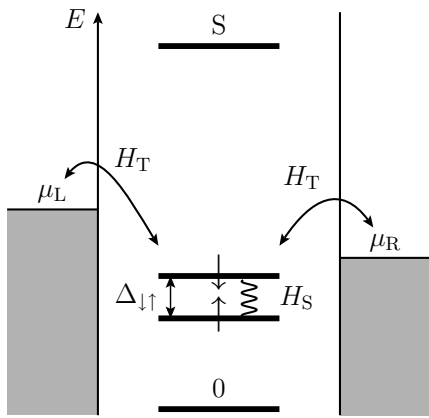


FIG. 1: Sketch of the quantum dot coupled via the tunneling Hamiltonian  $H_T$  to two leads at electro-chemical potentials  $\mu_L$  and  $\mu_R$  and to a phonon bath via the spin-phonon coupling Hamiltonian  $H_S$ . The dot can be either empty (0), in one of the spin-directions  $\uparrow$  and  $\downarrow$ , which are split by the Zeeman energy  $\Delta_{\downarrow\uparrow}$ , or in the singlet state S.

$\Delta_{\downarrow\uparrow} = E_{\downarrow} - E_{\uparrow} = -g\mu_B B_z$  of the single-particle dot levels. Furthermore, due to electron-electron interaction, the simultaneous occupation of the dot by two electrons costs the additional energy  $U$ . The leads  $\ell = L, R$  are modeled as Fermi liquids, i.e., by non-interacting quasiparticles with energy  $\epsilon_{\ell\mathbf{k}}$ , where  $\mathbf{k}$  is the wave-vector and  $\sigma$  the spin. The number operator  $n_{\ell\mathbf{k}\sigma} = c_{\ell\mathbf{k}\sigma}^\dagger c_{\ell\mathbf{k}\sigma}$  for the corresponding state is defined in terms of the fermionic creation and destruction operators  $c_{\ell\mathbf{k}\sigma}^\dagger$  and  $c_{\ell\mathbf{k}\sigma}$ , respectively. Each lead is filled up to an electro-chemical potential  $\mu_\ell$ , and thus the mean occupation numbers obey the Fermi distributions  $f_\ell(\epsilon) = \{\exp[(\epsilon - \mu_\ell)/k_B T] + 1\}^{-1}$ . Here, an externally applied bias voltage  $V$  maps to a difference  $\mu_L - \mu_R = eV$ . In the present work, we consider transport across a singly-occupied dot in the cotunneling regime. This imposes the condition  $E_\sigma \ll \mu_\ell \ll E_\sigma + U$  for  $\sigma = \uparrow, \downarrow$  and  $\ell = L, R$ . The last term in Eq. (2) describes the phonons of the environment, which consist of a collection of modes characterized by a wave-vector  $\mathbf{q}$  with occupation numbers  $n_{\mathbf{q}} = a_{\mathbf{q}}^\dagger a_{\mathbf{q}}$ . Here, the bosonic operators  $a_{\mathbf{q}}^\dagger$  ( $a_{\mathbf{q}}$ ) create (destroy) a phonon in the mode  $\mathbf{q}$ . Note that for reasons of notational simplicity, a possible branch index has been suppressed here, but can be added in the end results. At equilibrium, the phonons are described by the Bose-distribution  $n_B(\epsilon) = [\exp(\epsilon/k_B T) - 1]^{-1}$ .

The coupling of the dot to the leads is modeled by the tunneling Hamiltonian

$$H_T = \sum_{\ell\mathbf{k}\sigma} T_{\ell\mathbf{k}} c_{\ell\mathbf{k}\sigma}^\dagger d_\sigma + \text{h.c.}, \quad (3)$$

where, for reasons of simplicity, we have assumed spin-independent tunnel matrix elements  $T_{\ell\mathbf{k}}$ . For later use, we introduce the corresponding tunneling rates (per spin-

direction)

$$\Gamma_\ell(\epsilon) = \frac{2\pi}{\hbar} \sum_{\mathbf{k}} |T_{\ell\mathbf{k}}|^2 \delta(\epsilon - \epsilon_{\ell\mathbf{k}}). \quad (4)$$

So far, except for the presence of two instead of one lead, the Hamiltonian corresponds to the one of the single-site Anderson model,<sup>24</sup> which has been extensively studied in the literature.<sup>25</sup>

Finally, we assume that the dot spin interacts with the phonon system via a spin-phonon coupling of the form

$$H_S = \sum_{\mathbf{q}} (M_{\mathbf{q},x} \sigma_x + M_{\mathbf{q},y} \sigma_y) (a_{\mathbf{q}} + a_{-\mathbf{q}}^\dagger). \quad (5)$$

In order to guarantee the hermiticity of the coupling Hamiltonian, the coefficients have to fulfil  $M_{\mathbf{q},i} = M_{-\mathbf{q},i}^*$  for all  $\mathbf{q}$  and  $i = x, y$ . Furthermore, we have introduced the spin operators  $\sigma_x = d_\uparrow^\dagger d_\uparrow + d_\downarrow^\dagger d_\downarrow$  and  $\sigma_y = i(d_\downarrow^\dagger d_\uparrow - d_\uparrow^\dagger d_\downarrow)$ . Again, we can characterize the coupling by a spectral density, which is defined as

$$D(\omega) = \frac{\pi}{\hbar} \sum_{\mathbf{q}} |M_{\mathbf{q},x} + iM_{\mathbf{q},y}|^2 \delta(\omega - \omega_{\mathbf{q}}). \quad (6)$$

Note that the coupling does not contain dephasing terms proportional to  $\sigma_z = d_\uparrow^\dagger d_\uparrow - d_\downarrow^\dagger d_\downarrow$  or to the total number of electrons  $n = n_\uparrow + n_\downarrow$  on the dot. For the electron spin in a quantum dot this is justified to a very good approximation, as was shown in Ref. 17. In this regard, the present model differs, e.g., from the so-called Anderson-Holstein model,<sup>26,27</sup> which only contains coupling terms of this kind.

### III. SCHRIEFFER-WOLFF TRANSFORMATION

Since we are interested in transport in the cotunneling regime where the dot occupancy is only changed virtually, it is advantageous to eliminate to lowest order the tunneling Hamiltonian  $H_T$ , which changes the number of electrons on the dot by one. A standard method to achieve this goal is the so-called Schrieffer-Wolff transformation,<sup>28</sup> which we generalize to the case where a spin-flip coupling  $H_S$  is present. Accordingly, we perform the canonical transformation to the Hamiltonian

$$\bar{H} = e^S H e^{-S} = H_0 + H_S + \frac{1}{2} [S, H_T] + \mathcal{O}(H_T^3), \quad (7)$$

where the generator  $S$  of the transformation has to fulfil the condition  $[S, H_0 + H_S] + H_T = 0$ . In order to obtain an explicit expression for the generator  $S$ , we now use that, as has been discussed in the Introduction, in all relevant cases, the spin-flip coupling is weak and can be treated perturbatively. Hence, we can expand

$$S = L_0^{-1} H_T - L_0^{-1} [L_0^{-1} H_T, H_S] + \mathcal{O}(H_S^2). \quad (8)$$

Here,  $L_0$  is the Liouvillian of the decoupled dot, leads and phonon system.<sup>36</sup> We, thus, arrive at the transformed Hamiltonian

$$\bar{H} \approx H_0 + H_S + \frac{1}{2}[L_0^{-1}H_T, H_T] + \frac{1}{2}[L_0^{-1}[L_0^{-1}H_T, H_S], H_T]. \quad (9)$$

The first commutator corresponds to the standard Schrieffer-Wolff transformation<sup>28</sup> and yields a contribution

$$\frac{1}{2}[L_0^{-1}H_T, H_T] = H_{\text{dir,ex}} + H_{\text{ren}} + H_{2e}. \quad (10)$$

Here, the first term contains the direct and exchange interaction between the dot and the leads

$$H_{\text{dir,ex}} = \frac{1}{2} \sum_{\ell\ell'\mathbf{k}\mathbf{k}'\sigma\alpha} \frac{T_{\ell\mathbf{k}}T_{\ell'\mathbf{k}'}}{\epsilon_{\ell\mathbf{k}} - E_\sigma^\alpha} (n_\sigma^\alpha c_{\ell\mathbf{k}\sigma}^\dagger c_{\ell'\mathbf{k}'\sigma} - \alpha d_\sigma^\dagger d_\sigma c_{\ell\mathbf{k}\sigma}^\dagger c_{\ell'\mathbf{k}'\bar{\sigma}}) + \text{h.c.} \quad (11)$$

We denote flipped spins by  $\bar{\uparrow} = \downarrow$  and vice versa. Here and in the following, the sums over  $\alpha$  run over  $\alpha = \pm 1$ . Furthermore, we have introduced the abbreviations  $n_\sigma^\alpha = (1 - \alpha)/2 + \alpha n_\sigma$  and  $E_\sigma^\alpha = E_\sigma + [(\alpha + 1)/2]U$ . The next contribution to Eq. (10) is the renormalization of the dot Hamiltonian  $H_0$ ,

$$H_{\text{ren}} = \sum_{\ell\mathbf{k}\sigma\alpha} \frac{|T_{\ell\mathbf{k}}|^2}{\epsilon_{\ell\mathbf{k}} - E_\sigma^\alpha} n_\sigma^\alpha n_\sigma. \quad (12)$$

As this contribution can be absorbed in the definition of  $H_0$ , it will be ignored in the following. The last term, which describes processes that change the electron number on the dot by two, reads

$$H_{2e} = \frac{1}{2} \sum_{\ell\ell'\mathbf{k}\mathbf{k}'\sigma\alpha} \alpha \frac{T_{\ell\mathbf{k}}T_{\ell'\mathbf{k}'}}{\epsilon_{\ell\mathbf{k}} - E_\sigma^\alpha} d_\sigma d_\sigma c_{\ell'\mathbf{k}'\bar{\sigma}}^\dagger c_{\ell\mathbf{k}\sigma}^\dagger + \text{h.c.} \quad (13)$$

Later, we shall focus on the sector of the Hilbert space where the dot is singly occupied, and hence  $H_{2e}$  can be neglected, as well.

Similarly, we can decompose the phonon-mediated contributions to the transformed Hamiltonian (9) into

$$\frac{1}{2}[L_0^{-1}[L_0^{-1}H_T, H_S], H_T] = H_{\text{dir,ex}}^{\text{ph}} + H_{\text{ren}}^{\text{ph}} + H_{2e}^{\text{ph}}. \quad (14)$$

Here, the relevant contribution containing direct and exchange terms reads

$$H_{\text{dir,ex}}^{\text{ph}} = \frac{1}{2} \sum_{\ell\ell'\mathbf{k}\mathbf{k}'\sigma\alpha} T_{\ell\mathbf{k}} T_{\ell'\mathbf{k}'}^* X_{\ell\mathbf{k}\sigma\alpha} \times \left( n_\sigma^\alpha c_{\ell\mathbf{k}\sigma}^\dagger c_{\ell'\mathbf{k}'\bar{\sigma}} - \alpha d_\sigma^\dagger d_\sigma c_{\ell\mathbf{k}\sigma}^\dagger c_{\ell'\mathbf{k}'\sigma} \right) + \text{h.c.} \quad (15)$$

where we have introduced the phonon operator

$$X_{\ell\mathbf{k}\sigma\alpha} = \sum_{\mathbf{q}, i=x,y} \frac{M_{\mathbf{q},i} \sigma_i^{\sigma\bar{\sigma}}}{\epsilon_{\ell\mathbf{k}} - E_\sigma^\alpha} \left( \frac{a_{\mathbf{q}}}{\epsilon_{\ell\mathbf{k}} - E_\sigma^\alpha - \hbar\omega_{\mathbf{q}}} + \frac{a_{-\mathbf{q}}^\dagger}{\epsilon_{\ell\mathbf{k}} - E_\sigma^\alpha + \hbar\omega_{\mathbf{q}}} \right). \quad (16)$$

Furthermore, the transformation leads to a renormalization of the spin-phonon coupling

$$H_{\text{ren}}^{\text{ph}} = -\frac{1}{2} \sum_{\ell\mathbf{k}\sigma} |T_{\ell\mathbf{k}}|^2 X_{\ell\mathbf{k}\sigma} d_\sigma^\dagger d_\sigma + \text{h.c.} \quad (17)$$

Finally, a two-electron tunneling term

$$H_{2e}^{\text{ph}} = \frac{1}{2} \sum_{\ell\ell'\mathbf{k}\mathbf{k}'\sigma\alpha} \alpha T_{\ell\mathbf{k}} T_{\ell'\mathbf{k}'} X_{\ell\mathbf{k}\sigma\alpha} d_\sigma d_\sigma c_{\ell'\mathbf{k}'\sigma}^\dagger c_{\ell\mathbf{k}\sigma}^\dagger + \text{h.c.} \quad (18)$$

is generated, which, for the same reasons as above, will be disregarded together with the renormalization term (17).

#### IV. CURRENT

The mean current  $I_\ell(t)$  across contact  $\ell = \text{L, R}$  is given by the expectation value of the time-derivative of the total number of electrons  $N_\ell = \sum_{\mathbf{k}\sigma} n_{\ell\mathbf{k}\sigma}$  in lead  $\ell$  multiplied by the electron charge  $-e$ , i.e.,

$$I_\ell(t) = -e \langle \dot{N}_\ell \rangle = -\frac{ie}{\hbar} \langle [\bar{H}, N_\ell] \rangle. \quad (19)$$

For the evaluation of this expectation value, we switch to the interaction picture to obtain<sup>29,30</sup>

$$I_\ell(t) = \frac{ie}{\hbar} \int_0^{t-t_0} d\tau \langle [\tilde{N}_\ell(t-t_0), \tilde{H}_1(t-\tau-t_0)] \rangle. \quad (20)$$

Here, the tilde denotes interaction picture operators with respect to  $H_0$  and  $H_1 := \bar{H} - H_0$  is the coupling part of the effective Hamiltonian and the expectation value has to be taken at time  $t - \tau - t_0$ .

In the long-time limit  $t \gg t_0$ , the mean value of the current becomes time-independent and we find that due to charge conservation  $I_L = -I_R$ . Hence, we can write the total current as  $I = I_{\text{RL}} - I_{\text{LR}}$ , where  $I_{\ell\ell'}$  is the contribution of the electrons flowing from lead  $\ell$  into lead  $\ell'$ . In the cotunneling regime, where  $E_\sigma \ll \mu_\ell \ll E_\sigma + U$  for  $\sigma = \uparrow, \downarrow$  and  $\ell = \text{L, R}$ , the dot is, up to exponentially small corrections, always occupied by a single electron and hence is characterized by the occupation probabilities  $p_\sigma = \langle n_\sigma \rangle$  with  $p_\uparrow + p_\downarrow = 1$ . The currents  $I_{\ell\ell'}$  can then be written as<sup>23,31</sup>

$$I_{\ell\ell'} = e \sum_{\sigma\sigma'} W_{\ell'\sigma'\ell\sigma} p_\sigma, \quad (21)$$

where  $W_{\ell'\sigma'\ell\sigma}$  is the rate for an electron tunneling from lead  $\ell$  into lead  $\ell'$  when the dot was initially in the state  $\sigma$  and is in the state  $\sigma'$  afterwards. By convention, a process with  $\sigma' = \sigma$  is called *elastic* cotunneling, while the case with  $\sigma' = \bar{\sigma}$  is referred to as *inelastic* cotunneling.<sup>22</sup>

The contribution due to the cotunneling without participation of phonons to the rates  $W_{\ell'\sigma'\ell\sigma}$  will be designated by  $W_{\ell'\sigma'\ell\sigma}^{(0)}$ . In addition, the phonon-assisted cotunneling process contributes with rates  $W_{\ell'\sigma'\ell\sigma}^{(1)}$  to the

total rates  $W_{\ell'\sigma'\ell\sigma} = W_{\ell'\sigma'\ell\sigma}^{(0)} + W_{\ell'\sigma'\ell\sigma}^{(1)}$ . In the next two subsection, we discuss these two contributions in detail. Note that we thereby restrict ourselves to temperatures above the Kondo temperature, where correlations between the dot spin and the collective spin of the electrons in the lead do not play a role. We shall come back to a brief discussion of the low-temperature behavior in Sec. VIII.

### A. Elastic and inelastic cotunneling

Evaluating the current expression (20) for the direct and exchange terms (11), we arrive at the elastic cotunneling rate

$$W_{\ell'\sigma\ell\sigma}^{(0)} = \frac{\hbar}{2\pi} \int d\epsilon \Gamma_{\ell'}(\epsilon) \Gamma_{\ell}(\epsilon) \Lambda_{\sigma}^{(0),\text{el}}(\epsilon) f_{\ell}(\epsilon) [1 - f_{\ell'}(\epsilon)] \quad (22)$$

with  $\Lambda_{\sigma}^{(0),\text{el}}(\epsilon) = (E_{\bar{\sigma}} + U - \epsilon)^{-2} + (E_{\sigma} - \epsilon)^{-2}$ . Similarly, the inelastic cotunneling rate is given by

$$W_{\ell'\bar{\sigma}\ell\sigma}^{(0)} = \frac{\hbar}{2\pi} \int d\epsilon \Gamma_{\ell'}(\epsilon - \Delta_{\bar{\sigma}\sigma}) \Gamma_{\ell}(\epsilon) \Lambda_{\sigma}^{(0),\text{inel}}(\epsilon) \times f_{\ell}(\epsilon) [1 - f_{\ell'}(\epsilon - \Delta_{\bar{\sigma}\sigma})], \quad (23)$$

where  $\Lambda_{\sigma}^{(0),\text{inel}}(\epsilon) = [(E_{\bar{\sigma}} + U - \epsilon)^{-1} - (E_{\bar{\sigma}} - \epsilon)^{-1}]^2$ . In the inelastic case, the energy  $\Delta_{\bar{\sigma}\sigma}$  is deposited in or extracted from the dot. Correspondingly, the initial energy  $\epsilon$  of the tunneling electron coming from lead  $\ell$  differs by the same amount from the final energy of the electron in lead  $\ell'$ . Inelastic cotunneling is, thus, strongly suppressed for temperatures and external voltages much smaller than  $\Delta_{\bar{\sigma}\sigma}$ .

To a very good approximation, the energy dependence of the coupling rates  $\Gamma_{\ell}(\epsilon)$  can be ignored in the energy range contributing to the integrals in the rate expressions (22) and (23). Furthermore, near one of the resonances, e.g., for  $E_{\sigma} \lesssim \mu_{\ell} \ll E_{\bar{\sigma}} + U$ , we can expand the dominant energy denominator of  $\Lambda_{\sigma}^{(0),\text{el}}(\epsilon)$  and  $\Lambda_{\sigma}^{(0),\text{inel}}(\epsilon)$ , respectively, and carry out the energy integration.<sup>37</sup> This yields the approximate rates

$$W_{\ell'\sigma'\ell\sigma}^{(0)} \approx \frac{\hbar \Gamma_{\ell} \Gamma_{\ell'}}{2\pi} \frac{1}{\Delta_{\ell'\sigma'\ell\sigma}^2} \left\{ 1 + \frac{1}{4\Delta_{\ell'\sigma'\ell\sigma}^2} \times \left[ 4\pi^2 (k_{\text{B}}T)^2 + (\mu_{\ell'\ell} + \Delta_{\sigma'\sigma})^2 \right] \right\} \Theta(-\mu_{\ell'\ell} - \Delta_{\sigma'\sigma}) \quad (24)$$

where we have introduced the function

$$\Theta(\epsilon) = \frac{\epsilon}{1 - \exp(-\epsilon/k_{\text{B}}T)} \quad (25)$$

as well as the energies

$$\Delta_{\ell'\sigma'\ell\sigma} = \frac{E_{\sigma'} - \mu_{\ell'} + E_{\sigma} - \mu_{\ell}}{2} \quad (26)$$

and  $\mu_{\ell'\ell} = \mu_{\ell'} - \mu_{\ell}$ . Here, terms of the order  $\mathcal{O}([\max(k_{\text{B}}T, |\mu_{\ell'\ell} + \Delta_{\sigma'\sigma}|)/\Delta_{\ell'\sigma'\ell\sigma}]^4)$  have been neglected in the curly brackets.

### B. Phonon-assisted elastic and inelastic cotunneling

We now come to the current contributions due to the presence of the spin-phonon coupling. Using  $H_{\text{dir,ex}}^{\text{ph}}$  from Eq. (15), we obtain after a straightforward but lengthy calculation the rates for the phonon-assisted elastic cotunneling

$$W_{\ell'\sigma\ell\sigma}^{(1)} = \frac{\hbar}{8\pi^2} \int d\epsilon' \Gamma_{\ell'}(\epsilon') \int d\epsilon \Gamma_{\ell}(\epsilon) \Lambda_{\text{el}}^{(1)}(\epsilon, \epsilon') \times N(\epsilon - \epsilon') f_{\ell}(\epsilon) [1 - f_{\ell'}(\epsilon')]. \quad (27)$$

The corresponding energy denominator

$$\Lambda_{\text{el}}^{(1)}(\epsilon, \epsilon') = \sum_{\sigma} \left[ \frac{1}{(E_{\sigma} + U - \epsilon)(E_{\bar{\sigma}} + U - \epsilon')} + \frac{1}{(E_{\sigma} - \epsilon)(E_{\bar{\sigma}} - \epsilon')} \right]^2 \quad (28)$$

now depends on both the energy before and after the phonon emission and/or absorption. Note that as explained above, we use the term ‘‘elastic’’ only to indicate that the dot state before and after the cotunneling process is identical. From the point of view of the electron system, the phonon-mediated cotunneling process is, of course, no longer elastic. Rather, the electrons either emit the energy  $\epsilon - \epsilon'$  due to the stimulated and spontaneous emission of phonons or absorb the energy  $\epsilon' - \epsilon$  from the phonon system. Both processes are captured by the function

$$N(\Delta\epsilon) = D(\Delta\epsilon/\hbar) [n_{\text{B}}(\Delta\epsilon) + 1] + D(-\Delta\epsilon/\hbar) n_{\text{B}}(-\Delta\epsilon). \quad (29)$$

Similarly, we obtain the ‘‘inelastic’’ phonon-mediated cotunneling rates

$$W_{\ell'\bar{\sigma}\ell\sigma}^{(1)} = \frac{\hbar}{8\pi^2} \int d\epsilon' \Gamma_{\ell'}(\epsilon') \int d\epsilon \Gamma_{\ell}(\epsilon) \Lambda_{\text{inel}}^{(1)}(\epsilon, \epsilon') \times N(\epsilon - \epsilon' - \Delta_{\bar{\sigma}\sigma}) f_{\ell}(\epsilon) [1 - f_{\ell'}(\epsilon')] \quad (30)$$

with

$$\Lambda_{\text{inel}}^{(1)}(\epsilon, \epsilon') = \sum_{\sigma} \left[ \frac{1}{(E_{\sigma} + U - \epsilon)(E_{\sigma} + U - \epsilon')} - \frac{1}{(E_{\sigma} - \epsilon)(E_{\sigma} - \epsilon')} \right]^2. \quad (31)$$

For the further evaluation of the rate formulas we again assume energy-independent dot-lead couplings  $\Gamma_{\ell}$ . Since the energy denominators in Eqs. (28) and (31) are already of fourth order in  $\Delta_{\sigma\mu}$ , we can neglect their energy

dependence around  $\epsilon = \epsilon' = \mu$  to get a result valid to the same order as in Eq. (24). Carrying out one of the energy integrals, we obtain the approximate result for both rates

$$W_{\ell'\sigma'\ell\sigma}^{(1)} \approx \frac{\hbar\Gamma_\ell\Gamma_{\ell'}}{8\pi^2} \left( \frac{1}{\Delta_{\sigma'\ell}^2 \Delta_{\sigma\ell'}^2} + \frac{1}{\Delta_{\sigma'\ell}^2 \Delta_{\sigma\ell'}^2} \right) \times \int d\Delta\epsilon N(\Delta\epsilon) \Theta(-\mu_{\ell'\ell} - \Delta_{\sigma'\sigma} - \Delta\epsilon) \quad (32)$$

with the energy differences  $\Delta_{\sigma\ell} = E_\sigma - \mu_\ell$ . We now consider a spectral density of the spin-phonon coupling of the form

$$D(\omega \geq 0) = \gamma \hbar \omega_c^{1-s} \omega^s \quad (33)$$

with the dimensionless spin-phonon coupling parameter  $\gamma$ , the cut-off frequency  $\omega_c$  and an exponent  $s$ , which depends on the nature of the coupling. In order for our master-equation approach to be valid, we have to restrict ourselves to exponents  $s \geq 1$ . The exponent  $s = 1$  corresponds to the so-called Ohmic case, and below, we will find  $s = 3$  or  $s = 5$  for a spin-orbit mediated coupling to phonons. Inserting the spectral density (33) into Eq. (32), we can write the rates as

$$W_{\ell'\sigma'\ell\sigma}^{(1)} \approx \gamma (\hbar\omega_c)^{1-s} \frac{\hbar\Gamma_\ell\Gamma_{\ell'}}{8\pi^2} \left( \frac{1}{\Delta_{\sigma'\ell}^2 \Delta_{\sigma\ell'}^2} + \frac{1}{\Delta_{\sigma'\ell}^2 \Delta_{\sigma\ell'}^2} \right) \times (k_B T)^{1+s} J_s(-(\mu_{\ell'\ell} + \Delta_{\sigma'\sigma})/k_B T) \Theta(-\mu_{\ell'\ell} - \Delta_{\sigma'\sigma}) \quad (34)$$

with

$$J_s(a) = \frac{1 - e^{-a}}{a} \int_0^\infty dx \operatorname{sgn}(\ln x) \frac{|\ln x|^s \ln x + a}{x - 1} \frac{1}{x - e^{-a}}. \quad (35)$$

In the interesting cases of  $s = 1, 3$  and  $5$ , we find for the integral

$$J_1(a) = \frac{1}{6} (4\pi^2 + a^2) \quad (36)$$

$$J_3(a) = \frac{1}{60} (4\pi^2 + a^2) (8\pi^2 + 3a^2), \quad (37)$$

$$J_5(a) = \frac{1}{42} (2\pi^2 + a^2) (4\pi^2 + a^2) (8\pi^2 + a^2). \quad (38)$$

In the general case, one can readily show that  $J_s(a)$  is an even function, i.e.,  $J_s(a) = J_s(-a)$  for all  $s$  and  $a$ .

## V. MASTER EQUATION

For the evaluation of the current expressions given in the previous section, we still need the occupation probabilities  $p_\sigma$ . Their dynamics is governed by the master equation<sup>32</sup>

$$\dot{p}_\sigma = -W_{\sigma\sigma} p_\sigma + W_{\sigma\bar{\sigma}} p_{\bar{\sigma}} \quad (39)$$

with the total rates  $W_{\sigma\sigma} = W_{\sigma\sigma}^{\text{cot}} + W_{\sigma\sigma}^{\text{flip}}$ . Here,  $W_{\sigma\sigma}^{\text{cot}} = \sum_{\ell\ell'} W_{\ell'\bar{\sigma}\ell\sigma}$  is the spin-flip rate due to inelastic cotunneling, which, in contrast to the current formula (21), also contains processes involving a single lead only. Furthermore, spin-flip processes due to the spin-phonon coupling (5) have to be taken into account in the master equation (39). These processes lead to the additional rate

$$W_{\sigma\sigma}^{\text{flip}} = \frac{2}{\hbar} N(\Delta_{\sigma\bar{\sigma}}). \quad (40)$$

In the stationary limit, the solution of the master equation is given by  $p_\sigma = [1 + W_{\sigma\sigma}/W_{\sigma\bar{\sigma}}]^{-1}$ , where we have used the normalization condition  $p_\uparrow + p_\downarrow = 1$ . Note that since elastic cotunneling leaves the dot state invariant, besides the spin-flip rate  $W_{\sigma\sigma}^{\text{flip}}$  only the rates for the inelastic cotunneling processes appear in the master equation.

Figure 2 shows the ratio  $p_\uparrow/p_\downarrow$  of the populations as a function of the bias voltage  $V$  in the presence of an Ohmic environment for different coupling strengths  $\gamma$ . Near thermal equilibrium, i.e., for voltages far below the onset of inelastic cotunneling, i.e.,  $eV \ll |\Delta_{\downarrow\uparrow}|, k_B T$ , the total rates and thus the populations fulfil the detailed balance relation  $p_{\bar{\sigma}}/p_\sigma = W_{\sigma\sigma}/W_{\sigma\bar{\sigma}} = \exp(-\Delta_{\sigma\bar{\sigma}}/k_B T)$ . For higher bias voltages, inelastic cotunneling leads to a population of the excited dot state, i.e., a heating of the dot. This heating effect becomes less pronounced in the presence of the spin-phonon coupling, where the relaxation due to the rate (40) equilibrates the system. For a quantitative estimate of the heating effect, we consider the deviation  $h$  of the population ratio from its equilibrium value:

$$h = \left| \frac{p_\uparrow}{p_\downarrow} - \exp(\Delta_{\downarrow\uparrow}/k_B T) \right|. \quad (41)$$

Using the detailed balance relation for the rates  $W_{\sigma\sigma}^{\text{flip}}$ , we then find

$$h = \frac{|\exp(\Delta_{\downarrow\uparrow}/k_B T) - W_{\downarrow\downarrow}^{\text{cot}}/W_{\downarrow\uparrow}^{\text{cot}}|}{1 + W_{\uparrow\downarrow}^{\text{flip}}/W_{\downarrow\uparrow}^{\text{cot}}}. \quad (42)$$

Thus, even for a non-zero difference in the numerator, the heating effect becomes suppressed for  $W_{\uparrow\downarrow}^{\text{flip}} \gg W_{\downarrow\uparrow}^{\text{cot}}$ . In Fig. 2, we indicate the onset voltages of the heating regime, defined by the relation  $W_{\uparrow\downarrow}^{\text{flip}} = W_{\downarrow\uparrow}^{\text{cot}}$  by vertical dashed lines.

Finally, we remark that heating effects are suppressed when the dot-lead coupling is asymmetric,<sup>23</sup> say  $\Gamma_L \gg \Gamma_R$ . In this case the excitation of the dot, which is dominated by processes involving the tunneling from one lead to the other and which, hence, is proportional to the product  $\Gamma_L \Gamma_R$ , is negligible compared to the relaxing effects resulting from the coupling to the left lead, which are proportional to  $\Gamma_L^2$ . Such a situation may occur, e.g., when measuring the current through an atom or molecule on a surface which is contacted on one side by an STM tip<sup>10</sup> (cf. also discussion at the end of Sec. VII).

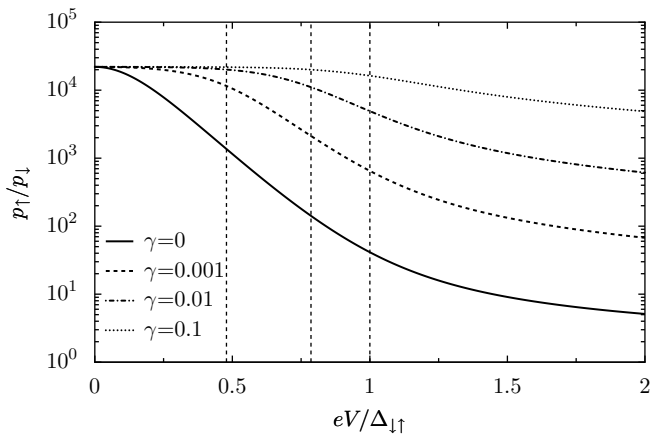


FIG. 2: Ratio  $p_{\uparrow}/p_{\downarrow}$  of the populations as a function of the bias voltage  $V$  in the presence of an Ohmic bath with different coupling strengths  $\gamma$ . The parameters are  $\Delta_{\downarrow\uparrow} = 0.1E_0$ ,  $T = 0.01E_0$  and  $\hbar\Gamma_L = \hbar\Gamma_R = 0.02E_0$ . Here,  $E_0 = |E_1 - \mu|$  is the energy difference between the energy  $E_1 = E_{\uparrow} = E_{\downarrow}$  of the degenerate dot level and the Fermi energy  $\mu = \mu_L = \mu_R$  in the leads in the absence of both the magnetic field and the bias voltage. The dashed vertical lines indicate the onset of the heating regime defined by  $W_{\uparrow\downarrow}^{\text{flip}} = W_{\uparrow\downarrow}^{\text{cot}}$ .

## VI. DIFFERENTIAL CONDUCTANCE

Having all the information for the evaluation of the current (21) at hand, we can now turn to the experimentally relevant quantity, the differential conductance  $g = dI/dV$ . As a function of the bias voltage, this quantity shows a characteristic step at the onset of inelastic cotunneling around  $|\Delta_{\downarrow\uparrow}|/e$ , when another transport channel becomes accessible. It is known that the width of this step is proportional to the temperature  $T$ , while

the broadening of the dot states due to their coupling to the leads does not play a role. Compared to a measurement in the sequential tunneling regime, an experiment can thus achieve a much higher precision for the determination of the splitting  $\Delta_{\downarrow\uparrow}$  (see Refs. 10 and 12). An open question, however, is how spin-flip processes taking place during the cotunneling process affect such a measurement.

Let us first consider the zero-temperature case without heating where the dot is always in its ground state which we assume to be the spin-up state. Evaluating the current using the approximate cotunneling rates (24) and (34), we then find for the contribution due to elastic cotunneling

$$g_{\text{el}} = \frac{e^2 \hbar \Gamma_L \Gamma_R}{2\pi \Delta_{L\uparrow R\uparrow}^2} \left\{ 1 + \frac{1}{4\Delta_{L\uparrow R\uparrow}^2} [4\pi^2 (k_B T)^2 + 3(eV)^2] + \frac{\gamma (\hbar\omega_c)^{1-s}}{4\pi} \left( \frac{\Delta_{L\uparrow R\uparrow}^2}{\Delta_{\downarrow L}^2 \Delta_{\uparrow R}^2} + \frac{\Delta_{L\uparrow R\uparrow}^2}{\Delta_{\uparrow L}^2 \Delta_{\downarrow R}^2} \right) \times (k_B T)^s [k_B T J_s(eV/k_B T) + eV J'_s(eV/k_B T)] \right\}, \quad (43)$$

where  $J'_s(a) = dJ_s(a)/da$ . In order to obtain a compact expression for the inelastic cotunneling current, we furthermore assume positive voltages  $V > 0$  and not too high temperatures  $k_B T \ll \Delta_{\downarrow\uparrow}$ . Then only the tunneling from the left to the right contact is relevant, i.e., the total current  $I$  is to a very good approximation given by  $I_{\text{RL}}$ . Furthermore, away from the step around  $V \approx \Delta_{\downarrow\uparrow}/e$ , we can use that up to exponentially small corrections  $\Theta(\epsilon) \approx 0$  for  $\epsilon \ll k_B T$  and  $\Theta(\epsilon) \approx \epsilon$  for  $\epsilon \gg k_B T$ . Thus, for  $eV \ll \Delta_{\downarrow\uparrow}$ , the inelastic cotunneling current vanishes and for voltages  $eV \gg \Delta_{\downarrow\uparrow}$ , it contributes with

$$g_{\text{inel}} = \frac{e^2 \hbar \Gamma_L \Gamma_R}{2\pi \Delta_{L\downarrow R\uparrow}^2} \left\{ 1 + \frac{1}{4\Delta_{L\downarrow R\uparrow}^2} [4\pi^2 (k_B T)^2 + 3(eV - \Delta_{\downarrow\uparrow})^2] + \frac{\gamma (\hbar\omega_c)^{1-s}}{4\pi} \left( \frac{\Delta_{L\downarrow R\uparrow}^2}{\Delta_{\uparrow L}^2 \Delta_{\uparrow R}^2} + \frac{\Delta_{L\downarrow R\uparrow}^2}{\Delta_{\downarrow L}^2 \Delta_{\downarrow R}^2} \right) (k_B T)^s [k_B T J_s((eV - \Delta_{\downarrow\uparrow})/k_B T) + (eV - \Delta_{\downarrow\uparrow}) J'_s((eV - \Delta_{\downarrow\uparrow})/k_B T)] \right\} \quad (44)$$

to the differential conductance. Particularly interesting is the step in between, which is centered around  $V = \Delta_{\downarrow\uparrow}/e$ . In order to obtain an estimate for its width  $\Delta V_{\text{step}}$ , we determine the onset  $V_{\text{on}}$  of inelastic cotunneling by using a linear approximation of the differential conductance around the center of the step,  $g(V) \approx g(\Delta_{\downarrow\uparrow}/e) + g'(\Delta_{\downarrow\uparrow}/e)(V - \Delta_{\downarrow\uparrow}/e)$  and intersecting with the purely elastic cotunneling curve (43) (see Fig. 3):  $g_{\text{el}}(V_{\text{on}}) = g(\Delta_{\downarrow\uparrow}/e) + g'(\Delta_{\downarrow\uparrow}/e)(V_{\text{on}} - \Delta_{\downarrow\uparrow}/e)$ . Approximately, we

can determine the solution of this non-linear equation by employing a linear approximation for the elastic cotunneling curve around the center of the step. Doing so, we obtain  $V_{\text{on}} = \Delta_{\downarrow\uparrow}/e - g_{\text{inel}}(\Delta_{\downarrow\uparrow}/e)/g'_{\text{inel}}(\Delta_{\downarrow\uparrow}/e)$ . Defining

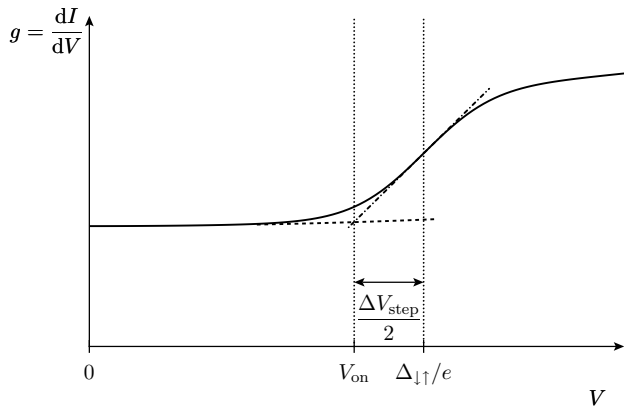


FIG. 3: Sketch of the procedure employed for the determination of the onset  $V_{\text{on}}$  and of the width  $\Delta V_{\text{step}}$  of the inelastic-cotunneling step. The dashed line shows the extrapolation of the differential conductance curve below the step. The dash-dotted line corresponds to the linear approximation of the step shape.

the width as twice the difference  $V_{\text{on}} - \Delta_{\downarrow\uparrow}/e$  gives

$$\Delta V_{\text{step}} = \frac{6k_{\text{B}}T}{e} \left\{ 1 - 3 \left( \frac{k_{\text{B}}T}{\Delta_{\text{L}\downarrow\text{R}\uparrow}} \right)^2 \left[ 1 + \gamma \frac{1}{6\pi} \times \left( \frac{\Delta_{\text{L}\downarrow\text{R}\uparrow}^4}{\Delta_{\uparrow\text{L}}^2 \Delta_{\uparrow\text{R}}^2} + \frac{\Delta_{\text{L}\downarrow\text{R}\uparrow}^4}{\Delta_{\downarrow\text{L}}^2 \Delta_{\downarrow\text{R}}^2} \right) \times (3J_s''(0) + 2J_s'(0)) \left( \frac{k_{\text{B}}T}{\hbar\omega_c} \right)^{s-1} \right] \right\}. \quad (45)$$

As mentioned above, the width is essentially proportional to the temperature. We also find that the spin-flip processes only modify the higher-order corrections in  $k_{\text{B}}T/\Delta_{\text{L}\downarrow\text{R}\uparrow}$ . Here, the spin-flip coupling contribution is proportional to  $\gamma$  and to a positive prefactor of the order of one and has a temperature dependence which depends on the ratio of thermal and cutoff energy. In fact, we find that with increasing coupling constant  $\gamma$  the width of the inelastic cotunneling step becomes reduced.

We now turn to the discussion of the heating effects by taking into account the stationary probability distribution according to the master equation (39). Figure 4 shows the differential conductance as a function of the voltage in the presence of an Ohmic spin-flip coupling of strength  $\gamma$ . In the upper panel, the case of a symmetric dot-lead coupling is depicted. As discussed above, this is the situation where heating effects are most relevant, and for  $\gamma = 0$  we indeed observe a noticeable deviation from the step-like behavior for voltages  $V \gtrsim \Delta_{\downarrow\uparrow}/e$ . With increasing spin-flip coupling strength  $\gamma$ , however, the dot is driven to equilibrium and the overshooting of the differential conductance curve disappears. As mentioned at the end of Sec. V, heating effects are suppressed when the dot-lead coupling is strongly asymmetric. Such a situation is shown in panel (b) of Fig. 4. In this case, the influence of the spin-phonon coupling is much weaker.

For larger voltages, the effect of phonon-assisted inelastic cotunneling becomes visible, as can be inferred from the inset of panel (b).

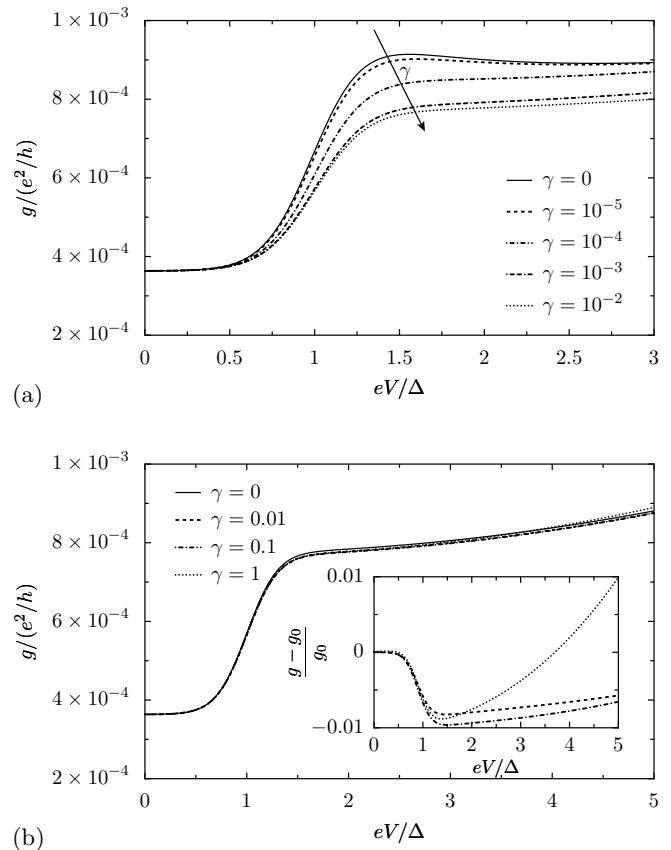


FIG. 4: Cotunneling conductance  $g$  as a function of the bias voltage  $V$  in the presence of an Ohmic bath with different coupling strengths  $\gamma$ . The parameters are  $\Delta_{\downarrow\uparrow} = 0.1E_0$ ,  $T = 0.01E_0$  and (a)  $\hbar\Gamma_{\text{L}} = \hbar\Gamma_{\text{R}} = 0.02E_0$ , (b)  $\hbar\Gamma_{\text{L}} = 0.002E_0$  with  $E_0$  as defined in the caption of Fig. 2. In the inset of panel (b), the relative difference between the differential conductance  $g$  in the presence of the spin-phonon coupling and the differential conductance  $g_0$  without spin-phonon coupling is depicted.

In Fig. 5, the step-width defined by the onset of inelastic cotunneling is shown as a function of the spin-flip coupling strength  $\gamma$  for different ratios  $\Gamma_{\text{L}}/\Gamma_{\text{R}}$ . For equal coupling to both leads, the main effect again comes from the suppression of the heating with increasing  $\gamma$ . The inset of Fig. 5 depicts the  $\gamma$ -dependence for larger  $\gamma$ . As described by the analytical expression (45) the width drops linearly. Due to the finite temperature, there is a slight offset compared to the full solution, however.

## VII. COMPARISON WITH EXPERIMENTS

We now apply the general results to the specific experimental situation of Ref. 12 and analyze the relevance of spin-phonon coupling effects in this case. In

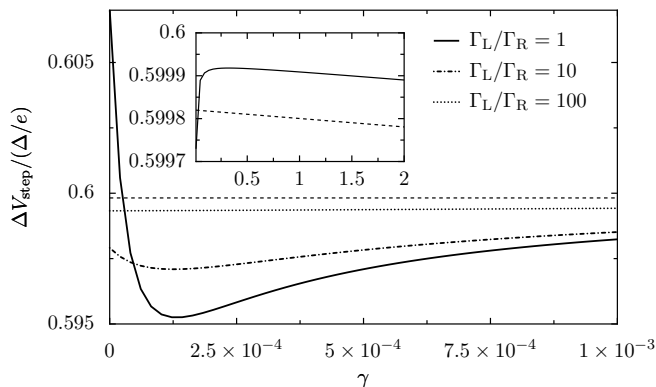


FIG. 5: Step width  $\Delta V_{\text{step}} = 2g'_{\text{inel}}(\Delta_{\downarrow\uparrow}/e)/g_{\text{inel}}(\Delta_{\downarrow\uparrow}/e)$  as a function of the coupling strength  $\gamma$  to an Ohmic bath for different ratios of the tunneling rates  $\Gamma_{L,R}$ , where the product  $\hbar^2\Gamma_L\Gamma_R = (0.02E_0)^2$  is kept constant. The other parameters are like in Fig. 4. The horizontal dashed line shows the width according to Eq. (45) for  $\gamma = 0$ . In the inset, the behavior for larger  $\gamma$  is shown together with the step width without heating according to Eq. (45) (dashed).

order to do so, we model the 2D quantum dot by an isotropic parabolic lateral confinement characterized by the frequency  $\omega_0$  in the absence of a magnetic field. In a magnetic field  $B_z$  perpendicular to the two-dimensional electron gas (2DEG), the relevant frequencies then are  $\omega_{1,2} = \Omega \mp \omega_c/2$  with the cyclotron frequency  $\omega_c = |e|B_z/m^*c$ , where  $m^*$  is the effective electron mass and  $\Omega = \sqrt{\omega_0^2 + \omega_c^2/4}$  corresponding to the effective lateral confinement length  $l = \sqrt{\hbar m^*/\Omega}$  (for more details, we refer the reader to Ref. 18). The parameters for the GaAs quantum dot of Ref. 12 are  $g = -0.16$ ,  $m^* = 0.067m_e$ ,  $B_z = 11\text{T}$  and we assume  $\hbar\omega_0 = 1.1\text{meV}$ .

We consider the influence of both Rashba<sup>33</sup> and Dresselhaus<sup>34</sup> spin-orbit coupling, which are characterized by spin-orbit lengths  $\lambda_R = \lambda_D = 8\mu\text{m}$  (see Appendix A). For a piezoelectric coupling to longitudinal and transversal phonon modes in the limit  $\omega \ll c_\alpha \min(\ell, d)$ , where  $d \approx 5\text{nm}$  is the vertical confinement length, the spectral density (33) of the spin-phonon coupling is cubic, i.e.,  $s = s_{\text{PE}} = 3$ . The prefactors for the longitudinal and transverse contributions are given by

$$\gamma_{\text{PE,L}} = \frac{Q_D^2 + Q_R^2}{70\pi\hbar\varrho c_L^3} \left( \frac{eh_{14}}{\kappa} \right)^2 \quad (46)$$

$$\gamma_{\text{PE,T}} = \frac{Q_D^2 + Q_R^2}{105\pi\hbar\varrho c_T^3} \left( \frac{eh_{14}}{\kappa} \right)^2 \quad (47)$$

with the speed of sound  $c_L = 4.73 \times 10^5 \text{cm/s}$  and  $c_T = 3.35 \times 10^5 \text{cm/s}$  of the longitudinal and transversal acoustic phonon modes, respectively. The density of GaAs is  $\varrho = 5.319 \text{g/cm}^3$  and the electron-phonon coupling parameters are  $eh_{14} = 1.2 \times 10^7 \text{eV/cm}$  and  $\kappa = 13.2$ . The spin-orbit coupling strength enters via

the dimensionless coupling constants<sup>17,18</sup>

$$Q_{R,D} = \frac{l}{\lambda_{R,D}} \left[ -\frac{\hbar\omega_1}{\hbar\omega_1 \mp \Delta_{\downarrow\uparrow}} + \frac{\hbar\omega_2}{\hbar\omega_2 \pm \Delta_{\downarrow\uparrow}} \right]. \quad (48)$$

The cut-off frequencies for the piezo-electric coupling are given by  $\omega_{c,\text{PE,L}} = c_L/l$  and  $\omega_{c,\text{PE,T}} = c_T/l$ . Note that the leading contribution to  $Q_{R,D}$  is linear in  $B_z$ , and consequently the rate (40) is proportional to  $B_z^5$  for low magnetic fields  $B_z$ .

In the case of a deformation potential coupling to acoustic phonons, the spectral density is proportional to  $\omega^5$ , i.e.,  $s = s_{\text{DA}} = 5$ , and the prefactor is given by

$$\gamma_{\text{DA}} = \frac{\Xi_0^2 (Q_D^2 + Q_R^2)}{24\pi\hbar\varrho l^2 c_L^3} \quad (49)$$

with  $\Xi_0 = 6.7 \text{eV}$ . The cut-off is at the frequency  $\omega_{c,\text{DA}} = c_L/l$ . Taking into account the magnetic-field-dependence of the prefactor  $\gamma_{\text{DA}}$ , the leading contribution to the rate (40) is proportional to  $B_z^7$  at low magnetic fields. Thus, the spin-phonon coupling due to the deformation potential electron-phonon interaction is only relevant for rather high magnetic fields. Furthermore, we take a temperature  $T = 15 \text{mK}$  and dot-lead coupling rates  $\hbar\Gamma_L = \hbar\Gamma_R = 17.5 \mu\text{eV}$  from Ref. 12. Finally, we assume a value  $|E_1 - \mu| = 0.4 \text{meV}$ , where  $E_1$  and  $\mu$  are the energy of the degenerate dot-level and the Fermi energy, respectively, in the absence of the bias voltage and the magnetic field. An external bias is assumed to drop symmetrically across both contacts.

Figure 6 depicts the differential conductance as a function of the bias voltage for the given set of parameters. Comparing the result of the calculation including the spin-orbit induced spin-phonon coupling (solid line) with the one without this coupling (crosses), we can conclude that these effects play a negligible role in the experiment by Kogan et al. However, as shown in the inset of Fig. 6, by reducing the dot-lead coupling by a bit more than one order of magnitude, one reaches a regime where the equilibration of the dot due to the spin-phonon coupling becomes relevant. As discussed in Sec. V, the transition to this regime is determined by the relation  $W_{\uparrow\downarrow}^{\text{flip}} = W_{\uparrow\downarrow}^{\text{cot}}$ , which for  $eV \gtrsim \Delta_{\downarrow\uparrow}$  yields the tunneling rate

$$\Gamma_{\text{on,heat}} = |\Delta_{L\downarrow R\uparrow}| \sqrt{\frac{2\pi W_{\uparrow\downarrow}^{\text{flip}}}{\hbar\Theta(eV - \Delta_{\downarrow\uparrow})}}. \quad (50)$$

This relation can be employed for the determination of the spin-flip rate  $W_{\uparrow\downarrow}^{\text{flip}}$  by means of a cotunneling transport measurement. In order to do so, one has to determine the critical tunneling rate  $\Gamma_{\text{on,heat}}$  marking the transition between the regime of the dot being in equilibrium and the one where heating effects are relevant. As an indicator for this transition one can measure the ratio of the differential conductance above and below the inelastic cotunneling step. Determining this quantity as a function of the dot-lead coupling strength yields  $\Gamma_{\text{on,heat}}$

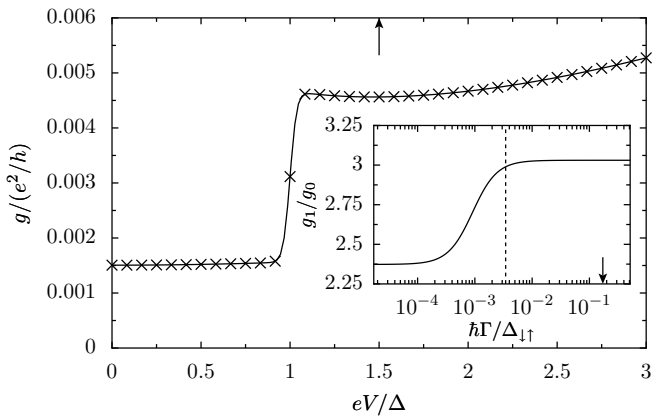


FIG. 6: Differential conductance  $g$  as a function of the bias voltage  $V$  for the parameters given in the main text. The crosses show the result in the absence of the spin-phonon coupling. In the inset, the ratio of the differential conductance  $g_1$  at  $V_1 = 1.5\Delta_{\downarrow\uparrow}/e$  (see arrow in the main panel) and the differential conductance  $g_0$  at zero voltage for different values of the dot-lead coupling rates  $\Gamma = \Gamma_L = \Gamma_R$ . The dashed vertical line designates the value given by Eq. (50) and the arrow the dot-lead coupling rate in the experiment<sup>12</sup>.

(cf. inset of Fig. 6) and via Eq. (50) the spin-flip rate  $W_{\uparrow\downarrow}^{\text{flip}}$ .

Let us finally discuss whether such a measurement scheme would also apply to transport experiments through single atoms or molecules on a surface, e.g., the ones reported in Ref. 10. There, the tunnel-coupling to the two leads is strongly asymmetric, one contact being via the insulating surface and the other via an STM tip. As has been discussed at the end of Sec. V, heating effects are suppressed in this case. Indeed, the form of the differential conductance-voltage characteristics seen in Ref. 10 can—above the Kondo temperature—be very well described by an equilibrium probability distribution of the spin state of the atom. However, for a not too small tunnel-coupling across the insulating layer, it should be possible to enter the heating regime by adjusting the atom-tip coupling strength appropriately. If this coupling strength is not too far away from the critical value given by Eq. (50), it should be possible to measure the intrinsic spin-relaxation rate due to phonons by using a similar scheme as the one proposed above, although only the atom-STM coupling strength can be controlled easily. On the other hand, it is in principle feasible to control the molecule-surface coupling strength by modifying the chemical binding of the molecule to the surface, as was shown in Ref. 11, so the proposed scheme could be applied to such a situation, as well.

### VIII. SCALING BEHAVIOR

So far, we have restricted the discussion to the case of temperatures well above the so-called Kondo-

temperature  $T_K$ . For lower temperatures, correlations between between the dot spin and a collective spin degree of freedom of the electrons in the leads become important and a perturbative treatment of the problem breaks down. This leads to the so-called Kondo effect, which has been analyzed in great detail in the literature for the Anderson model<sup>25</sup>. We now briefly discuss the effect of additional spin-flip processes due to the term  $H_S$  using the poor man's scaling approach put forward by Anderson<sup>35</sup>. In order to keep the discussion as simple as possible, we consider a simplified version of our effective Hamiltonian (9), which ignores the lead-, momentum- and spin-dependence of the coupling constants as well as the direct interaction between the lead states:

$$\begin{aligned} \bar{H} = H_0 - JS_{\text{d}} \cdot \mathbf{s} + J_S (XS_{\text{d}}^x + YS_{\text{d}}^y) \\ - J_1 (XS_{\text{d}}^x + YS_{\text{d}}^y) n(0) + J_2 (Xs^x + Ys^y) \end{aligned} \quad (51)$$

Here, we have introduced the spin operators

$$\mathbf{s} = \frac{1}{2} \sum_{\ell\ell'\mathbf{k}\mathbf{k}'\sigma\sigma'} c_{\ell\mathbf{k}\sigma}^\dagger \boldsymbol{\tau}_{\sigma\sigma'} c_{\ell'\mathbf{k}'\sigma'} \quad \text{and} \quad (52)$$

$$\mathbf{S}_{\text{d}} = \frac{1}{2} \sum_{\sigma\sigma'} d_{\sigma}^\dagger \boldsymbol{\tau}_{\sigma\sigma'} d_{\sigma'}, \quad (53)$$

where  $\boldsymbol{\tau}$  is the vector consisting of the three Pauli matrices. The density of lead electrons at the position of the dot is given by

$$n(0) = \sum_{\ell\ell'\mathbf{k}\mathbf{k}'\sigma} c_{\ell\mathbf{k}\sigma}^\dagger c_{\ell'\mathbf{k}'\sigma}. \quad (54)$$

The phonon operators are defined as  $X = \sum_{\mathbf{q}} M_{\mathbf{q},x} (a_{\mathbf{q}} + a_{-\mathbf{q}}^\dagger)$  and  $Y = \sum_{\mathbf{q}} M_{\mathbf{q},y} (a_{\mathbf{q}} + a_{-\mathbf{q}}^\dagger)$ .

During the scaling procedure, contributions due to excitations of electrons and holes far away from the Fermi energy  $\mu = 0$ , at a cutoff energy  $\pm D$ , are successively integrated out. If the resulting effective interaction is again of the form (51), we can absorb it in the coupling constants. Note that in general, the coupling constants thereby acquire a momentum dependence. However, as long as the cutoff energy is still large enough, this dependence can be ignored for the relevant states near the Fermi energy. Doing so, we obtain the usual scaling equations for the exchange constant  $J$ :

$$\frac{dJ}{dD} = -2\nu \frac{J^2}{D}, \quad (55)$$

which, in particular, is not influenced by the other terms in the Hamiltonian (51). The renormalization of the electron-phonon coupling constant is given by

$$\frac{dJ_S}{dD} = \nu J J_2 \sum_{\ell\mathbf{k}}^{|e_{\ell\mathbf{k}}| < D} \frac{1}{D + |e_{\ell\mathbf{k}}|} = (4 \ln 2) \nu^2 J J_2 \quad (56)$$

while the coupling constants  $J_1$  and  $J_2$  remain invariant. Here,  $\nu$  is the density of states in the leads. In

the anti-ferromagnetic case, where  $J > 0$  scales to  $\infty$  as  $D \rightarrow 0$ , the same holds true for the spin-phonon coupling constant  $J_S$ . We conclude that far away from the active region around the Fermi energy, neither the pure spin-flip term proportional to  $J_S$  nor the phonon-assisted tunneling terms, i.e., the last two terms in the Hamiltonian (51), modify the scaling behavior of the Kondo-type coupling of the dot spin to the leads.

## IX. CONCLUSIONS

We have theoretically studied the influence of a spin-phonon coupling on the cotunneling through a nanoscale system. By means of a Schrieffer-Wolff transformation, we have derived an explicit Hamiltonian in which the relevant cotunneling processes appear to lowest order. This allowed us to evaluate the rates for elastic and inelastic cotunneling in the presence of spin-flip processes. We found that the width of the inelastic cotunneling step is only weakly influenced by the spin-flip processes. More important are the relaxation effects of the spin-phonon coupling which counteract the heating of the quantum dot due to inelastic cotunneling. Considering a realistic model for a recent experiment<sup>12</sup>, we propose a new way of determining the spin relaxation rate due to spin-phonon coupling in a cotunneling experiment.

### Acknowledgments

The authors thank D. Bulaev, W.A. Coish, V.N. Golovach, F. von Oppen, D. Saraga, and P. Simon for helpful discussion. Financial support by the EU RTN QuE-MolNa, the NCCR Nanoscience, the Swiss NSF, DARPA, ARO, and ONR is acknowledged.

### APPENDIX A: DERIVATION OF SPIN-PHONON COUPLING HAMILTONIAN

In this appendix, we derive the spin-phonon coupling (5) starting from a Hamiltonian describing an electron in a two-dimensional electron gas with an external magnetic field  $B_z$  in z-direction

$$H_0 = \frac{\mathbf{P}^2}{2m^*} + U(\mathbf{r}) + \frac{1}{2}g\mu_B B_z \sigma_z \quad (\text{A1})$$

where  $\mathbf{P} = \mathbf{p} + (|e|\hbar/c)\mathbf{A}(\mathbf{r})$  is the kinetic momentum,  $U(\mathbf{r})$  is the confinement potential, and  $\mathbf{A}(\mathbf{r}) = (B_z/2)(-y, x, 0)$  is the vector potential. For  $x, y, z$  pointing along the main crystallographic axes of the GaAs crystal, and the electron gas lying in the [001] plane, the spin-orbit interaction assumes the form

$$H_{\text{SO}} = H_{\text{D}} + H_{\text{R}} \quad (\text{A2})$$

with the Dresselhaus<sup>34</sup> and Rashba<sup>33</sup> contributions

$$H_{\text{D}} = \beta_{\text{D}}(-\sigma_x P_x + \sigma_y P_y), \quad H_{\text{R}} = \alpha_{\text{R}}(\sigma_x P_y - \sigma_y P_x). \quad (\text{A3})$$

The strength of the spin-orbit coupling is conveniently measured in terms of the spin-orbit lengths  $\lambda_{\text{D}} = \hbar/m^*\beta_{\text{D}}$  and  $\lambda_{\text{R}} = \hbar/m^*\alpha_{\text{R}}$ . Finally, the orbital degrees of freedom of the electron are coupled to the phonon system via the electron-phonon interaction  $H_{\text{e-ph}} = \sum_{\mathbf{q}} M_{\mathbf{q}}(\mathbf{r})(a_{\mathbf{q}} + a_{-\mathbf{q}}^\dagger)$ , where a branch index has been suppressed.

Applying to the Hamiltonian  $H = H_0 + H_{\text{SO}} + H_{\text{e-ph}}$  a Schrieffer-Wolff transformation which eliminates  $H_{\text{SO}}$  to lowest order and projecting on the orbital ground state, we obtain to lowest order the *spin-phonon* coupling

$$H_{\text{S}} = \langle 0|[S, H_{\text{e-ph}}]|0\rangle \quad (\text{A4})$$

where the generator  $S$  of the canonical transformation has to fulfil  $[S, H_0] = -H_{\text{SO}}$ . From Eqs. (A1)–(A3), we can infer that the generator can be written in the form  $S = i(A_x \sigma_x + A_y \sigma_y)$  with  $A_x$  and  $A_y$  being Hermitian operators which act on the orbital degrees of freedom only. Hence, we obtain

$$H_{\text{S}} = i\langle 0|[A_x, H_{\text{e-ph}}]|0\rangle \sigma_x + i\langle 0|[A_y, H_{\text{e-ph}}]|0\rangle \sigma_y. \quad (\text{A5})$$

Letting  $M_{\mathbf{q},i} = \langle 0|[\Omega_i, M_{\mathbf{q}}(\mathbf{r})]|0\rangle$  for  $i = x, y$ , we thus arrive at the coupling Hamiltonian (5).

For a quantum dot with parabolic lateral confinement (see Sec. VII), it is useful to choose coordinates rotated by 45° degrees around the  $z$ -axis<sup>17</sup>, i.e., we let  $x \rightarrow (x + y)/\sqrt{2}$  and  $y \rightarrow (y - x)/\sqrt{2}$ . In this new coordinate frame, the generator  $S$  of the canonical transformation is defined in terms of

$$A_x = \frac{\alpha_{\text{R}}}{2\Omega} \left[ \omega_1 \frac{m^*\Omega y + p_x}{\hbar\omega_1 - \Delta_{\downarrow\uparrow}} + \omega_2 \frac{m^*\Omega y - p_x}{\hbar\omega_2 + \Delta_{\downarrow\uparrow}} \right] + \frac{\beta_{\text{D}}}{2\Omega} \left[ \omega_1 \frac{m^*\Omega y + p_x}{\hbar\omega_1 + \Delta_{\downarrow\uparrow}} + \omega_2 \frac{m^*\Omega y - p_x}{\hbar\omega_2 - \Delta_{\downarrow\uparrow}} \right], \quad (\text{A6})$$

$$A_y = \frac{\alpha_{\text{R}}}{2\Omega} \left[ \omega_1 \frac{-m^*\Omega x + p_y}{\hbar\omega_1 - \Delta_{\downarrow\uparrow}} + \omega_2 \frac{-m^*\Omega x - p_y}{\hbar\omega_2 + \Delta_{\downarrow\uparrow}} \right] + \frac{\beta_{\text{D}}}{2\Omega} \left[ \omega_1 \frac{m^*\Omega x - p_y}{\hbar\omega_1 + \Delta_{\downarrow\uparrow}} + \omega_2 \frac{m^*\Omega x + p_y}{\hbar\omega_2 - \Delta_{\downarrow\uparrow}} \right]. \quad (\text{A7})$$

Note that this transformation diverges for magnetic field strengths with  $\hbar\omega_{1,2} \pm \Delta_{\downarrow\uparrow} = 0$ . A detailed analysis of the relaxation rates in this case can be found in Ref. 18. On the other hand, for  $|\Delta_{\downarrow\uparrow}| \ll \hbar\omega_{1,2}$ , the leading contribution to the relaxation rates comes from the terms linear in  $\Delta_{\downarrow\uparrow} \propto B_z$  (see Ref. 17).

- 
- \* Electronic address: joerg.lehmann@unibas.ch
- <sup>1</sup> D. D. Awschalom, D. Loss, and N. Samarth, *Semiconductor Spintronics and Quantum Computation* (Springer, Berlin, 2002).
  - <sup>2</sup> I. Zutic, J. Fabian, and S. Das Sarma, *Rev. Mod. Phys.* **76**, 323 (2004).
  - <sup>3</sup> M. A. Nielsen and I. L. Chuang, *Quantum Computation and Quantum Information* (Cambridge University Press, New York, 2000).
  - <sup>4</sup> V. Cerletti, W. A. Coish, O. Gywat, and D. Loss, *Nanotechnology* **16**, R27 (2005).
  - <sup>5</sup> R. Sessoli, D. Gatteschi, A. Caneschi, and M. A. Novak, *Nature* (London) **365**, 141 (1993).
  - <sup>6</sup> M. N. Leuenberger and D. Loss, *Nature* (London) **410**, 789 (2001).
  - <sup>7</sup> W. Liang, M. P. Shores, M. Bockrath, J. R. Long, and H. Park, *Nature* **417**, 725 (2002).
  - <sup>8</sup> F. Meier, J. Levy, and D. Loss, *Phys. Rev. Lett.* **90**, 047901 (2003).
  - <sup>9</sup> F. Troiani, M. Affronte, S. Carretta, P. Santini, and G. Amoretti, *Phys. Rev. Lett.* **94**, 190501 (2005).
  - <sup>10</sup> A. J. Heinrich, J. A. Gupta, C. P. Lutz, and D. M. Eigler, *Science* **306**, 466 (2004).
  - <sup>11</sup> A. Zhao, Q. Li, L. Chen, H. Xiang, W. Wang, S. Pan, B. Wang, X. Xiao, J. Yang, J. G. Hou, and Q. Zhu, *Science* **309**, 1542 (2005).
  - <sup>12</sup> A. Kogan, S. Amasha, D. Goldhaber-Gordon, G. Granger, M. A. Kastner, and H. Shtrikman, *Phys. Rev. Lett.* **93**, 166602 (2004).
  - <sup>13</sup> D. M. Zumbühl, C. M. Marcus, M. P. Hanson, and A. C. Gossard, *Phys. Rev. Lett.* **93**, 256801 (2004).
  - <sup>14</sup> S. I. Erlingsson and Y. V. Nazarov, *Phys. Rev. B* **66**, 155327 (2002).
  - <sup>15</sup> A. Khaetskii, D. Loss, and L. Glazman, *Phys. Rev. Lett.* **88**, 186802 (2002).
  - <sup>16</sup> W. A. Coish and D. Loss, *Phys. Rev. B* **70**, 195340 (2004).
  - <sup>17</sup> V. N. Golovach, A. Khaetskii, and D. Loss, *Phys. Rev. Lett* **93**, 016601 (2004).
  - <sup>18</sup> D. V. Bulaev and D. Loss, *Phys. Rev. B* **71**, 205324 (2005).
  - <sup>19</sup> T. Fujisawa, D. G. Austing, Y. Tokura, Y. Hirayama, and S. Tarucha, *Nature* (London) **419**, 278 (2002).
  - <sup>20</sup> J. M. Elzerman, R. Hanson, L. H. W. van Beveren, B. Witkamp, L. M. K. Vandersypen, and L. P. Kouwenhoven, *Nature* (London) **430**, 431 (2004).
  - <sup>21</sup> M. Kroutvar, Y. Ducommun, D. Heiss, M. Bichler, D. Schuh, G. Abstreiter, and J. J. Finley, *Nature* (London) **432**, 81 (2004).
  - <sup>22</sup> D. V. Averin and Y. V. Nazarov, *Phys. Rev. Lett.* **65**, 2446 (1990).
  - <sup>23</sup> V. N. Golovach and D. Loss, *Phys. Rev. B* **69**, 245327 (2004).
  - <sup>24</sup> P. W. Anderson, *Phys. Rev.* **124**, 41 (1961).
  - <sup>25</sup> A. C. Hewson, *The Kondo Problem to Heavy Fermions* (Cambridge University Press, Cambridge, 1993).
  - <sup>26</sup> T. Holstein, *Ann. Phys. (N.Y.)* **8**, 325 (1959).
  - <sup>27</sup> P. W. Anderson, *Phys. Rev. Lett.* **34**, 953 (1975).
  - <sup>28</sup> J. R. Schrieffer and P. A. Wolff, *Phys. Rev.* **149**, 491 (1966).
  - <sup>29</sup> G. D. Mahan, *Many-Particle Physics*, 3rd ed. (Plenum Press, New York, 2000).
  - <sup>30</sup> S. Kohler, J. Lehmann, and P. Hänggi, *Phys. Rep.* **406**, 379 (2005).
  - <sup>31</sup> E. V. Sukhorukov, G. Burkard, and D. Loss, *Phys. Rev. B* **63**, 125315 (2001).
  - <sup>32</sup> K. Blum, *Density Matrix Theory and Applications*, 2nd ed. (Plenum Press, New York, 1996).
  - <sup>33</sup> Y. L. Bychkov and É. I. Rashba, *Phis'ma Zh. Eksp. Theor. Fiz.* **39**, 66 (1984) [*JETP Lett.* **39**, 78 (1984)].
  - <sup>34</sup> G. Dresselhaus, *Phys. Rev.* **100**, 580 (1955).
  - <sup>35</sup> P. W. Anderson, *J. Phys. C* **3**, 2436 (1970).
  - <sup>36</sup> The Liouvillian superoperator  $L_0$  has vanishing diagonal matrix elements in the basis  $|n\rangle\langle n'|$ , where  $|n\rangle$  are the eigenstates of the Hamiltonian  $H_0$ . In order to obtain an invertible operator, one has to add an infinitesimal imaginary part.  $L_0^{-1}$  has to be understood in this sense. The resulting infinitesimal imaginary parts in the denominators of Eq. (11) and the like, are, however, not relevant for the following discussion.
  - <sup>37</sup> By expanding the energy denominators, we remove divergences at  $\epsilon = E_\sigma$  and  $\epsilon = E_\sigma + U$ , which are, however, exponentially suppressed in the cotunneling regime.